

Two new evolved bipolar planetary nebulae in the solar neighbourhood

David J. Frew,¹*† Quentin A. Parker^{1,2} and Delphine Russeil³

¹*Department of Physics, Macquarie University, NSW 2109, Australia*

²*Anglo-Australian Observatory, PO Box 296, Epping, NSW 1710, Australia*

³*LAM, 2 Place Le Verrier, 13248 Marseille Cedex 04, France*

Accepted 2006 August 3. Received 2006 July 28; in original form 2005 December 16

ABSTRACT

We present AAO/UKST H α + [N II] narrow-band imagery and low- and medium-resolution optical spectroscopy of RCW 24 and RCW 69. These nebulae were previously classified as H II regions, but we now show them to be two of the largest and nearest bipolar Type I PNe yet discovered. Distances were estimated using extinction–distance and kinematic methods, and via a new H α surface brightness–radius relation. The adopted distances are 1.0 ± 0.3 kpc for RCW 24 and 1.3 ± 0.2 kpc for RCW 69. Both objects have enhanced nitrogen abundances, with $\log N/O \simeq +0.44$ for RCW 24, and $\log N/O = +0.33$ for RCW 69. Systemic velocities and $|z|$ distances are $V_{\text{LSR}} = +5$ km s⁻¹ and $|z| \sim 23$ pc for RCW 24, and $V_{\text{LSR}} = -33$ km s⁻¹ and only $|z| \sim 7$ pc for RCW 69. Both PNe originated from massive progenitors (>2.0 – $2.5 M_{\odot}$), as deduced from their chemical abundances, large ionized masses, small $|z|$ distances, low peculiar velocities and relatively hot central stars. These two objects form an important addition to the small sample of evolved bipolar PNe in the solar neighbourhood.

Key words: stars: AGB and post-AGB – planetary nebulae: general – planetary nebulae: individual: RCW 24 – planetary nebulae: individual: RCW 69.

1 INTRODUCTION

Amongst the family of planetary nebulae (PNe), those with bipolar morphologies are amongst the most complex and least understood. Are bipolar PNe the product of single star or binary star evolution (Soker 1998; cf. Corradi & Schwarz 1995; hereafter CS95)? Are all bipolar PNe formed from higher mass progenitor stars? How are the bipolar symbiotic outflows (e.g. Corradi & Schwarz 1993; Corradi 1995; Corradi et al. 1999) related to these objects? A fuller understanding of the bipolar phenomenon awaits an accurately defined sample of such PNe with reliable distances, fluxes, masses, chemical abundances, kinematics and central star properties.

It is well known that strongly bipolar PNe usually show strongly enhanced He and N abundances (e.g. CS95). Greig (1967, 1971) first drew attention to the correlation between morphology and chemistry, before Peimbert & Serrano (1980; following Peimbert 1978) defined Type I PNe as those with $N(\text{He})/N(\text{H}) \geq 0.14$ or $\log N/O \geq 0$. Most of the Type I PNe then known had a filamentary (or bipolar) structure (Peimbert 1978). Peimbert & Torres-Peimbert (1983; hereafter PTP83) investigated a sample of 29 Type I PNe and found most of them to have bipolar morphologies. CS95 investigated a homogenous sample of 43 bipolar PNe and found that the class as a whole is typified by enhanced nitrogen, helium (and

neon) abundances, higher than average expansion velocities and linear diameters, hotter (and more massive) central stars (Tylenda 1989), a lower Galactic scaleheight (~ 130 pc) and smaller deviations from Galactic circular rotation. In summary, bipolar PNe appear to be derived from higher-mass progenitor stars (≥ 2.0 – $2.5 M_{\odot}$; Peimbert & Serrano 1980; Phillips 2001a), though CS95 adopted a more conservative lower limit of $1.5 M_{\odot}$. It is now generally accepted that more massive progenitors are needed to produce the enhanced He and N abundances seen in these objects (see Becker & Iben 1980; Kingsburgh & Barlow 1994, hereafter KB94; Iben 1995).

However, the proportion of bipolar outflows relative to the total population of PNe is at present only approximately known (CS95; Manchado et al. 1996; Phillips 2001b). Obviously a more complete sample of PNe emphasizing the evolved end of the PN luminosity function needs to be obtained before a volume-limited sample can be defined (e.g. Frew & Parker 2005). The recently completed AAO/UKST H α survey of the southern Galactic plane (Parker et al. 2005) is ideally placed to provide significant new statistical data on PNe, due to its combination of areal coverage, high sensitivity and arcsec resolution. The original 3-h exposure H α survey films and matching 15-min *R*-band exposures have been scanned with the SuperCOSMOS measuring machine at the Royal Observatory, Edinburgh (Hambly et al. 2001) and are now available online¹ as a digital data product (Parker et al. 2005).

*E-mail: dfrew@ics.mq.edu.au

†Present address: Perth Observatory, 337 Walnut Road, Bickley, WA 6076, Australia.

¹ See <http://www-wfau.roe.ac.uk/sss/halpha/>

A systematic visual search of the original H α films, as well as a complete examination of the SuperCOSMOS pixel data for all 233 survey fields at 16 \times blocked-down resolution, has so far yielded \sim 900 new PNe. A preliminary list was detailed in Version 1.0 of the Macquarie/AAO/Strasbourg/H α (MASH) Catalogue of Galactic Planetary Nebulae² originally available on CD-ROM (Parker et al. 2001, 2003). A complete, fully revised catalogue of identifications, images, spectroscopy and other parameters is now available (Parker et al. 2006).

Here we present AAO/UKST H α narrow-band imaging and confirmatory low- and medium-resolution spectroscopy of two newly identified, large evolved bipolar PNe, RCW 24 and RCW 69. Curiously, previous investigators had misidentified these large nebulosities as H II regions for more than four decades (Frew & Parker 2003). It is the improved morphological detail offered by the AAO/UKST H α survey, combined with new spectroscopic data and the identification of good central star candidates, that has led to our re-evaluation of their nature. These ‘new’ PNe are of large angular size and intrinsic diameter, making them two of the closest and most physically extended bipolar PNe known.

2 IDENTIFICATION

2.1 RCW 24

This unusually large PN was noted serendipitously from first-epoch ESO-*R* Sky Survey films by D. J. Frew in 1995, and was later reported as a possible new PN (Frew 1997) based on its unusual morphology, despite the then accepted H II identification. It was independently found on the AAO/UKST H α survey field h 458 (exposure HA 18308) by Q. A. Parker in 1998 as part of the MASH identification programme where it was more clearly identified as a probable evolved bipolar PN. Earlier, Brand, Blitz & Wouterloot (1986) noted it in their list of H II regions, which also includes several reflection nebulae and a sprinkling of PNe. They gave no further comment on its nature and the two lobes of the PN were each given separate designations (BRAN 147A/B).

In addition, a red image is presented by Neckel & Vehrenberg (1990), where it was again assumed to be an H II region. The object lies about 2.5 from the northern edge of the Vela SNR and about 1.5 from the western edge of the large H II region Gum 14 = RCW 27 (Gum 1955; Rodgers, Campbell & Whiteoak 1960a). Despite the strong and extensive nebulosity associated with the nearby Vela Molecular Ridge (Murphy & May 1991), the PN itself is set in a relatively quiescent region apart from a low level, relatively uniform ‘wash’ of galactic emission, as shown in the calibrated low-resolution Southern H α Sky Survey Atlas (SHASSA) images of Gaustad et al. (2001).

The SIMBAD data base plots the object RCW 24 a few arcmin to the south-west of our position, based on the coordinates listed by Rodgers et al. (1960a), but there is no obvious nebulous object at that position on H α survey field h 458. Careful examination of the relevant plate from the RCW atlas (Rodgers et al. 1960b) showed that the bipolar nebulosity is indeed present, and furthermore there is no visible object at their catalogued position. Acknowledging that positional errors of up to 5 arcmin are not unknown in the RCW catalogue (Rodgers et al. 1960a), we identify RCW 24 as an earlier observation of the two objects separately catalogued by Brand et al. (1986).

² Formerly called the Edinburgh/AAO/Strasbourg Catalogue

Table 1. Basic PN properties.

Name	RCW 24	RCW 69
MASH identifier	PHR0825-4013	PHR1244-6231
Other ID		Gum 45
	Bran 147 A/B	Bran 396
	Fr 1-1	Fr 1-2
PN	G258.5-01.3	G302.1+00.3
RA (J2000)	08 ^h 25 ^m 47 ^s .54	12 ^h 44 ^m 27 ^s .35
Dec. (J2000)	−40° 13′ 10″.3	−62° 31′ 17″.8
Dimensions (arcsec) ^a	615 \times 440	248 \times 221
Dimensions (arcsec) ^b	1320 \times 1080	320 \times 251

^aInner dimensions; ^bouter dimensions.

RCW 24 is readily visible on the standard UKST *R*-band survey image as two wedge-shaped lobes of emission, which extend about 10 arcmin. The lobes are symmetrically placed around an 18th-magnitude blue central star candidate that we subsequently identified (see Section 6). We quote a new position, taken as that of the central star candidate, in Table 1.

It is likely that the object’s large angular size, coupled with the faintness of the overall nebulosity on the previously available broad-band photographic images, mitigated against a previous PN identification. However, the deeper high-resolution AAO/UKST H α image (Fig. 1) has not only made the bipolarity of the prominent emission lobes self-evident, but has also revealed the PN’s fainter outer extensions for the first time. These extensions are about 22 \times 18 arcmin² in size, with the major axis oriented east–west.

2.2 RCW 69

This little-studied object was discovered by Gum (1955), who catalogued it as an H II region, and it was later noted by Rodgers et al. (1960a), Brand et al. (1986) and Neckel & Vehrenberg (1990), all of whom followed Gum’s H II region interpretation. It was considered

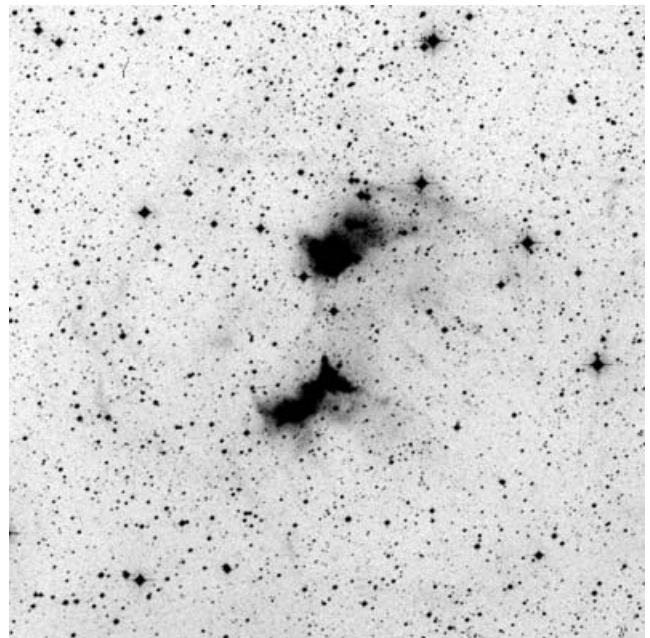


Figure 1. A 25 \times 25 arcmin² AAO/UKST H α survey image of RCW 24. Note the faint extensions are oriented east–west. NE is to the top left-hand side of this image.

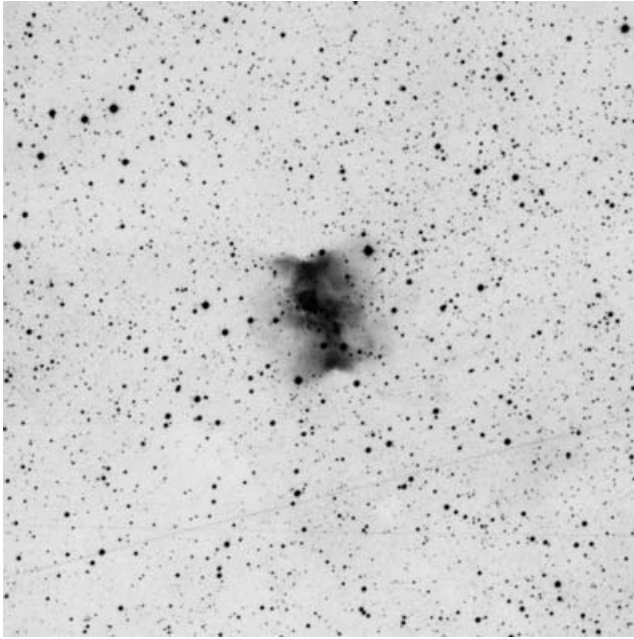


Figure 2. A 20×20 arcmin² AAO/UKST H α survey image of RCW 69. NE is to the top left-hand side.

to be a new possible PN by D. J. Frew in 1997, based on its appearance on ESO *R* and SERC *J* films, though an unambiguous classification could not be made at that time (Frew, unpublished). It was independently identified as a possible bipolar PN by Q. A. Parker around the same time, based on its appearance on AAO/UKST H α image h 136. It was hence designated PHR1244-6231 in an unpublished addendum to Parker et al. (2001). The deeper H α image, along with optical spectroscopy taken as part of the MASH survey (see Section 3), allowed us to confirm its identification as a new bipolar PN. Fig. 2 shows the H α image extracted from the online data of survey field h 136 (exposure HA 17901) scanned by SuperCOSMOS. A coherent bipolar or ‘butterfly’ morphology is seen, encapsulated within a fainter envelope of ~ 5 arcmin dimension. This object lies in a fairly quiescent region with no significant H II regions located within 30 arcmin.

The central bar of RCW 69 is oriented approximately north–south and is probably the projection of a thick nearly edge-on torus similar to that seen in M 76 (= NGC 650/1) and Sh 1-89 (Hua 1997). The bar has a mottled appearance in the H α + [N II] survey image and there is a hint that two emission knots show point symmetry. Some apparent sinuous dust lanes in the eastern half of the bar show that the foreground absorption is not uniform. Faint emission extends

perpendicularly east and west of the bar, and seems to represent bipolar outflows along the polar axis, though this feature is much fainter than the outflows seen in M 76 and Sh 1-89. The UKST *B_J* plate (which is primarily an [O III] image of the nebula) shows the bar as a low surface brightness elliptical haze of dimensions 215×130 arcsec², smaller and less well defined than on the red image. The basic properties of the two new PNe are given in Table 1.

3 SPECTROSCOPIC OBSERVATIONS

3.1 RCW 24

Low-resolution long-slit spectra were obtained for RCW 24 at the 1.9-m telescope of the South African Astronomical Observatory (SAAO) in 2003 January and 2004. The observations are summarized in Table 2. For all the SAAO observations, the standard grating spectrograph was used with the SITe 1798×266 pixel CCD. On-chip binning ($2 \times$) perpendicular to the dispersion direction was used to reduce readout noise. The slit width was $400 \mu\text{m}$ (~ 2.4 arcsec on the sky), and the slit length perpendicular to the dispersion direction was 100 arcsec, fixed in an east–west orientation. Grating #7 (300 lines/mm⁻¹) was used giving a spectral coverage of $3300\text{--}7300 \text{ \AA}$ at a resolving power of $R \approx 1000$. A range of spectrophotometric standard stars from the list of Stone & Baldwin (1983) were used to flux calibrate the SAAO spectra, and PN flux standards from Dopita & Hua (1997) were used as additional checks on the flux calibration and radial velocity determinations (Section 7.2). Dome screen flats and twilight flats were also obtained, with wavelength calibration being applied via Cu–Ar arc exposures bracketing the observations. The spectra were reduced and analysed using standard IRAF routines.

The slit was positioned to ensure that suitable sky regions were recorded on the CCD as the nebula would otherwise entirely fill the slit. It is clear from the size of RCW 24 relative to the slit length that very faint outer emission has been subtracted from the data, which may have slightly perturbed the [N II]/H α ratio of the spectra.

3.2 RCW 69

Low-resolution spectra of RCW 69 were obtained with the FLAIR II multi-object fibre spectrograph (Watson et al. 1993; Parker 1997) on the 1.2-m UKST in 1998 August (see Morgan & Parker 1998, for additional instrumental details). A 600 V grating was used, angled to cover the blue and red spectral regions, with sampling provided by $100\text{-}\mu\text{m}$ fibres (subtending 6.7 arcsec on the sky). The resolving power was $R \approx 1000$ and 1400 for the blue and red arms, respectively. Sky subtraction for the FLAIR spectra of RCW 69 used the median background from 10 dedicated sky fibres dispersed over the field,

Table 2. Summary of spectral observations.

Object ID	Telescope	Date observed	Dispersion lines (mm)	Coverage (\AA)	Exposure (s)
RCW 24	1.9-m SAAO	30/01/2003 ^a	300B	3250–7250	600
RCW 24	1.9-m SAAO	01/02/2003 ^b	300B	3250–7250	1200
RCW 24	1.9-m SAAO	14/02/2004 ^c	300B	3550–7500	1200
RCW 69	1.2-m UKST/FLAIR	11/08/1998	600V	4350–5780	4×1800
RCW 69	1.2-m UKST/FLAIR	11/08/1998	600V	5810–7220	3×1800
RCW 69	1.9-m SAAO	24/06/2003	1200R	6120–6870	1200
RCW 69	1.9-m SAAO	25/06/2003	300B	3250–7250	2×600

^aSouth lobe, 120-arcsec south of CS; ^bnorth lobe, 120-arcsec north of CS; ^ccentral star (CS).

Table 3. Reddening-corrected line intensities, $I(\lambda)$, flux ratios and logarithmic extinctions for RCW 24 and RCW 69.

ID	λ	$f(\lambda)$	RCW 24 (a)	RCW 24 (b)	RCW 69 (c)	RCW 69 (d)	RCW 69 (e)	RCW 69 (f)
[O II]	3727	0.257	*	275:	–	–	385	367
H γ	4340	0.127	*	42	–	–	–	*
He II	4686	0.043	50	16	30	–	34	51
H β	4861	0.000	100	100	100	–	100	100
[O III]	4959	–0.024	148	77	162	–	169	125
[O III]	5007	–0.036	346	184	456	–	388	351
[N I]	5199	–0.083	–	–	–	–	–	29
[N II]	5755	–0.195	–	30	–	–	–	26
He I	5876	–0.215	–	–	–	–	–	34
[O I]	6300	–0.282	–	52	–	–	–	32
[N II]	6548	–0.318	588	424	494	400	578	499
H α	6563	–0.320	286	286	286	286	286	286
[N II]	6583	–0.323	1597	1276	1649	1263	1791	1487
He I	6678	–0.336	–	–	–	8	–	–
[S II]	6716	–0.342	169	96	90	78	159	95
[S II]	6731	–0.344	72	49	71	61	119	91
[A III]	7136	–0.396	–	–	–	–	–	11
[O III]/H β	–	–	5.4	2.6	6.2	–	5.6	4.8
[N II]/H α	–	–	7.6	6.1	7.5	5.8	8.3	6.9
[S II]/H α	–	–	0.84	0.51	0.56	0.49	0.97	0.65
[S II] λ 6717/ λ 6731	–	–	2.3	2.0	1.27	1.28	1.34	1.04
c_β	–	–	0.20	0.13	–	–	0.64	0.87

Notes. (a) south lobe; (b) north lobe; (c) FLAIR; (d) 1200R grating; (e) 300B grating, first exposure and (f) 300B grating, second exposure.

and well away from the body of the nebula. These observations were part of an observing run for new PN candidates identified in H α survey field h 136 as part of the overall MASH spectroscopic follow-up project. The FLAIR spectra were reduced using the IRAF DOFIBERS package.

Low-resolution spectra were also obtained for RCW 69 at the 1.9-m SAAO telescope in 2003 June, along with medium dispersion spectra taken with Grating #5 (1200 lines mm^{–1}, blazed for the red spectral range), covering $\lambda\lambda$ 6100–7300 Å at $R \approx 5000$. The SAAO spectra were reduced using standard IRAF routines. The log of observations is summarized in Table 2. All SAAO and FLAIR spectra were centred on the brightest knot in the PN, located ≈ 25 arcsec east and 5 arcsec north of the central star (see below).

4 NEBULAR LINE INTENSITIES

The line intensities for both PNe are summarized in Table 3. The fluxes are normalized to H β = 100 and are corrected for reddening using the $R = 3.1$ Galactic reddening law of Howarth (1983). The observed logarithmic extinction was determined in the standard way using an intrinsic ratio of $I(\text{H}\alpha/\text{H}\beta) = 2.86$, appropriate for $T_e = 10^4$ K (Brocklehurst 1971). The observed line fluxes can be recovered by multiplying the corrected fluxes by $10^{-c_f(\lambda)}$ where the reddening function $f(\lambda)$ is given in column 3 of Table 3 for convenience. The line intensities of both PNe are summarized in Table 3.

4.1 RCW 24

The fluxes for individual spectral lines are given in Table 3. The intensities of the brighter lines are estimated to be accurate to better than ± 10 per cent, rising to ± 50 per cent for the faintest lines. Lines definitely present but too faint or noisy to be reliably measured are marked with an asterisk (*). The low-dispersion SAAO spectra show intense [N II] lines at $\lambda\lambda$ 6548, 6584 compared to H α , immediately suggesting classification as a Type I PN (see Section 9). RCW 24

falls in the evolved end of the PN regime in the H α /[S II] versus H α /[N II] diagnostic diagram of Riesgo-Tirado & López (2002). In its surface brightness, spectrum and overall morphology, it strongly resembles the bipolar Mask nebula (PN G321.6+02.2 = CVMP 1; Corradi et al. 1997; see also Lynga 1965). For ease of comparison an AAO/UKST H α survey image of the Mask nebula is included here as Fig. 3.

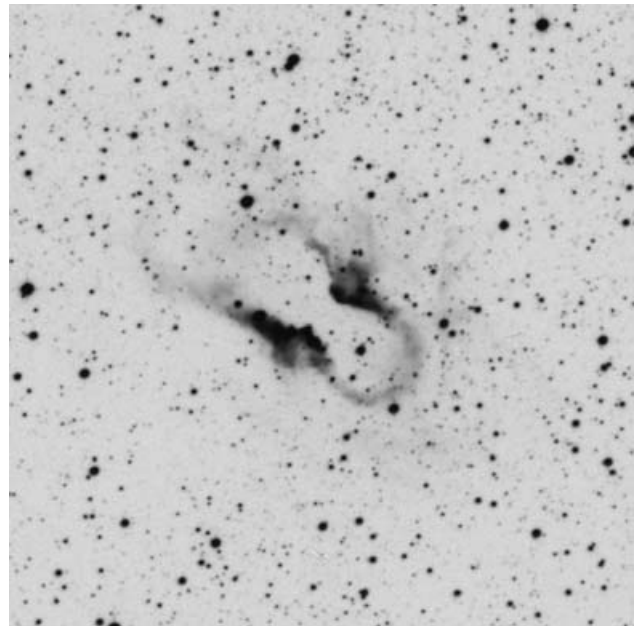


Figure 3. A 10×10 arcmin² AAO/UKST H α survey image of the ‘Mask’ nebula, PN G321.6+02.2 (Corradi et al. 1997). NE is to the top left-hand side. Note the strong similarity between this object (~ 2.0 kpc distant) and RCW 24, depicted in Fig. 1.

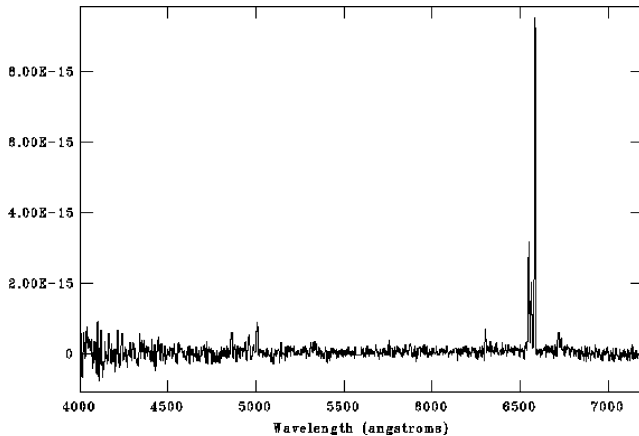


Figure 4. Flux-calibrated SAAO spectrum of the north lobe of RCW 24 obtained from a 1200-s low-dispersion exposure. Note the strength of the 6548 and 6583 Å [N II] lines relative to H α and [O III]. The ordinate gives the flux in cgs units.

The flux-calibrated spectrum of the SAAO spectrum across the cusp of the southern lobe of RCW 24 is given in Fig. 4. However, the low signal-to-noise ratio (S/N) of the [O III] and H β lines makes an accurate determination of the [O III]/H β (and hence the excitation class) rather difficult to obtain; the S/N in the blue of the northern lobe spectrum is worse. The very faint nebulosity around the central star is of lower excitation, with a [N II]/H α ratio of only $\sim 1.2 \pm 0.3$.

4.2 RCW 69

With FLAIR fibre spectra it is generally not possible to apply a reliable flux calibration due to the small fibre diameter. However, accurate line ratios for closely separated lines, such as the [N II] doublet and H α are readily derived, along with well-calibrated radial velocities. Like RCW 24, RCW 69 also exhibits intense [N II] lines; the two FLAIR spectra have [N II]/H $\alpha = 7.5 \pm 0.8$ and [O III]/H $\beta = 6.2 \pm 0.5$.

The 2003 June SAAO spectra confirm the very strong [N II] lines seen in the FLAIR spectra, with [N II]/H $\alpha \sim 7.0$ (see Fig. 5). When this is tied in to the larger angular extent and detailed morphology revealed by the H α survey data (Fig. 2), it is readily seen to be another

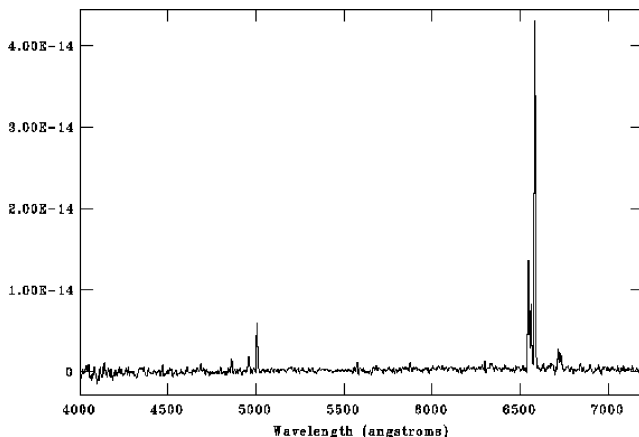


Figure 5. Flux-calibrated SAAO spectrum of RCW 69 obtained from a 600-s low-dispersion exposure. The spectrum is similar to that of RCW 24, though of somewhat higher excitation.

highly evolved Type I bipolar PN. This object plots close to RCW 24 in the H α /[S II] versus H α /[N II] diagnostic diagram of Riesgo-Tirado & López (2002). Our adopted value for the [N II]/H α ratio (with the FLAIR data given double weight) is ~ 7.2 (see Table 3). The averaged [O III]/H β ratio for all spectra was ~ 6.0 , which is more consistent with a medium excitation PN rather than a H II region. The Balmer decrement indicates it is moderately reddened, with the averaged logarithmic extinction at H β , $c = 0.76$. The derived colour excess and total visual absorption are $E(B - V) = 0.52 \pm 0.08$ and $A_V = 1.62 \pm 0.25$, attributed to its location behind the obscuring dust-clouds of the well-known Coalsack Nebula (see Section 7).

Copetti (2000) measured integrated H β and [O III] fluxes for RCW 69 through a 150-arcsec aperture covering the centre of the PN. It was assumed to be a H II region, despite the high measured [O III]/H β ratio of 8.6 ± 2.9 , which agrees, to within the errors, with the weighted average derived from our SAAO and FLAIR II spectra.

5 INTEGRATED FLUXES

Integrated H α fluxes for both RCW 24 and RCW 69 were determined from the SHASSA (Gaustad et al. 2001), which presents narrow band (H α + [N II]) and red continuum CCD images of the whole southern sky. SHASSA has a much lower spatial resolution (48-arcsec pixels) compared with the AAO/UKST H α survey (0.67-arcsec pixels) but has the benefit of being continuum subtracted and accurately flux calibrated. Despite the relatively coarse resolution of the SHASSA data, both PNe are large enough to be well resolved.

We obtained aperture photometry of RCW 24 and RCW 69 from SHASSA continuum-subtracted fields #77 and #34, respectively, using the APERPHOTOM routine in the Starlink GAIA image analysis package. As the SHASSA H α bandpass includes a contribution from the $\lambda\lambda 6548, 83$ [N II] lines, the SAAO and FLAIR spectra were used to deconvolve the [N II] contribution from the measured SHASSA red flux to calculate a H α flux only, knowing the transmission characteristics of the SHASSA filter (Gaustad et al. 2001). Both the quoted zero-point error in the SHASSA calibration of ~ 9 per cent and the estimated error in our adopted [N II]/H α ratio have been added in quadrature to the measured error in the SHASSA red flux (primarily due to counting statistics and variations in the background) to get the overall uncertainty in the H α flux for each PN. For RCW 24, we adopt [N II]/H $\alpha = 6.6 \pm 0.5$ (a weighted mean of the two ‘lobe’ spectra) and derive $\log F(\text{H}\alpha) = -10.95 \pm 0.08 \text{ erg cm}^{-2} \text{ s}^{-1}$ through a 14-arcmin aperture. For RCW 69, we estimate $\log F(\text{H}\alpha) = -10.91 \pm 0.06 \text{ erg cm}^{-2} \text{ s}^{-1}$ through a 7-arcmin aperture, after adopting [N II]/H $\alpha = 7.2 \pm 0.5$.

For RCW 69, Copetti (2000) measured $\log F(\text{H}\beta) = -12.04 \pm 0.12$ through a 2.5-arcmin aperture, so we derive $\log F(\text{H}\beta) = -11.65 \pm 0.15$ after scaling by a geometric factor up to the full dimensions of the PN, and hence determine $\log F(\text{H}\alpha) = -10.89 \pm 0.16$, using the observed Balmer decrement. This is in excellent agreement with the value determined here from the integrated SHASSA flux. For comparison purposes we also provide an integrated H α flux for CVMP 1 (not corrected for reddening) using the published [N II]/H α ratio given by Corradi et al. (1997). The derived value is $\log F(\text{H}\alpha) = -11.95 \pm 0.20$.

Integrated [O III] $\lambda 5007$ Å fluxes can also be estimated. Using an average observed [O III]/H β ratio from our spectra, we derive $F(5007) = -11.1 \pm 0.2$ for RCW 24 and $F(5007) = -11.0 \pm 0.2$ for RCW 69. This latter value is in excellent agreement with the scaled [O III] aperture flux for RCW 69 from Copetti (2000).

6 CENTRAL STARS

6.1 RCW 24

A faint blue central star (CSPN) has been found symmetrically placed between the two bipolar lobes of RCW 24 (Fig. 6). It is located at $\alpha, \delta = 08^{\text{h}}25^{\text{m}}47^{\text{s}}.54, -40^{\circ}13^{\text{m}}10^{\text{s}}.3$ (J2000) based on its coordinates from standard image parametrization (IAM) of SuperCOSMOS data (Hambly et al. 2001) of the UKST broad-band B_j and R plates. UBV images were kindly obtained by Dr Patrick Woudt with the SAAO 1.0-m reflector on the night of 2004 February 16, which gave $V = 18.21 \pm 0.03$, $B - V = 0.03 \pm 0.08$ and $U - B = -0.99 \pm 0.10$. The colours are consistent with a hot central star suffering some modest extinction. If the typical colour of an unreddened CSPN is $(B - V)_0 = -0.35 \pm 0.03$ (e.g. Kaler 1983; Bergeron, Wesemael & Beauchamp 1995) then $E(B - V) = 0.38 \pm 0.09$, higher than the reddening estimated from the Balmer decrement.

A SAAO spectrum of the central star was obtained on 2004 February 14. The spectrum is unfortunately of very low S/N, but none the less shows a steeply rising blue continuum and possible Balmer absorption lines. An uncertain absorption feature near $\lambda 4650 \text{ \AA}$ may be due to C IV. We refrain from quoting a spectral type at this stage; deeper spectra are needed to address this.

6.2 RCW 69

There is a pair of stars (11.1-arcsec separation in PA $\sim 90^\circ$) near the geometric centre of the RCW 69 (Fig. 6). The western star of the pair is closer to the symmetry axis of the PN and is a partially resolved double, as seen on the 2MASS J, H and K_s images. We have identified a bluish CSPN candidate ~ 5 arcsec SE of this star, based on UBV images obtained with the MSSSO 1.0-m reflector (see the right-hand panel in Fig. 6). The star is almost completely blended on the available SuperCOSMOS R -band and $H\alpha$ images, and is completely invisible on the 2MASS JHK_s images, despite the better resolution. It has a position of $\alpha, \delta = 12^{\text{h}}44^{\text{m}}27^{\text{s}}.35, -62^{\circ}31^{\text{m}}17^{\text{s}}.8$ (J2000) from direct measurement of the SuperCOSMOS B -band pixel data. As the sky conditions were non-photometric, only approximate magnitudes are estimated from the CCD frames, $U = 17.4 \pm 0.3$ and $B = 18.4 \pm 0.3$. No magnitude can be estimated from the available V -band image, so instead we assume $(B - V)_0 =$

-0.35 for a hot CSPN as before, and using the reddening from Section 4, estimate $V = 18.6 \pm 0.3$.

7 DISTANCE ESTIMATES

7.1 Extinction distances

RCW 24 lies in a relatively transparent region of the Galactic plane (at least for the first 1–2 kpc), making the derivation of a useful extinction–distance relation somewhat problematic (see below). For RCW 24 we adopt $E(B - V) = 0.30 \pm 0.10$, derived from the average of the nebular values, combined with the reddening estimate from the CS photometry. This value can be compared to the approximate asymptotic extinction through the plane in this direction of $E(B - V) = 2.51(A_v = 7.8 \text{ mag})$ as determined from the extinction map of Schlegel, Finkbeiner & Davis (1998). The most distant molecular cloud (G258.50–1.50) in this direction is at an inferred distance of 9.4 kpc (May, Alvarez & Bronfman 1997), showing the line of sight is extensive through the disc here. If we assume the edge of the disc is at $D \simeq 12$ kpc, this gives an average absorption of $0.75 \text{ mag kpc}^{-1}$.

Fitzgerald’s (1968) region at $l = 260.5$ includes the position of the PN, and shows little reddening out to 800 pc where a sudden increase to $E(B - V) = 0.6$ is seen, confirmed by the equivalent data of Neckel & Klare (1980), which shows $A_v = 1.8 \text{ mag}$ at 1.0 kpc. Lucke (1978) found near $l = 260^\circ$ an increase in colour excess between 0.5 and 1.0 kpc. This increase in reddening at 1.0 kpc is probably due to dust associated with the Vela Molecular Ridge (Murphy & May 1991; see also Pettersson & Reipurth 1994).

In an attempt to refine the reddening distance for RCW 24, a literature search for all stars using the SIMBAD data base was undertaken in a circular area of radius 45 arcmin centred on the PN. Spectroscopic parallaxes were determined by adopting the intrinsic colours and absolute magnitudes for each spectral class from Schmidt-Kaler (1982). Fig. 7 shows the extinction–distance diagram for the RCW 24 field, based on stars with the best-quality photometry and spectroscopy. There is too much scatter in this direction to define an unambiguous trend, and hence an accurate distance to the PN. However, a possible lower limit to the distance of 500 pc is indicated, based on the available data.

For RCW 69 the observed reddening is $E(B - V)$ of 0.52 ± 0.08 , due primarily to the foreground Coalsack nebula at a distance of

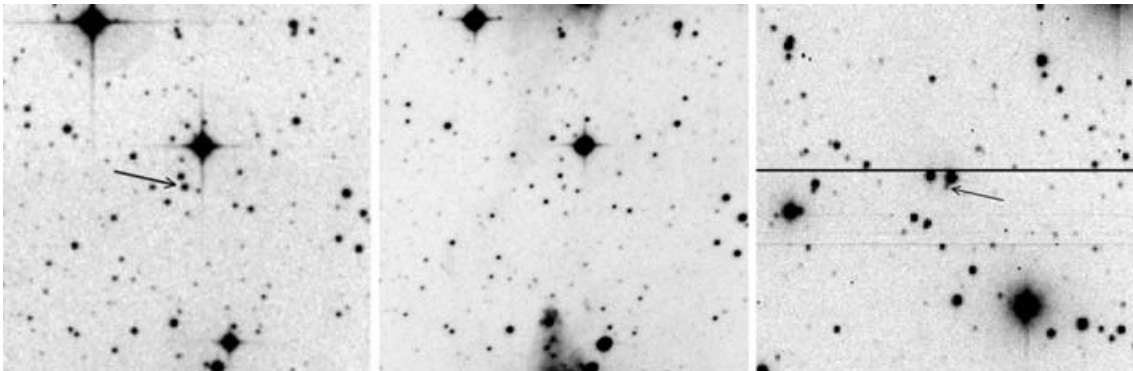


Figure 6. Left-hand and middle panels: 4×4 arcmin² extracts of SuperCOSMOS data of the B_j and $H\alpha$ images of the centre of RCW 24. The central star is identified at the end of the arrow (left-hand panel), and the cusps of the nebulous lobes are visible at the top and bottom of the red image (middle panel). Right-hand panel: Johnson B image of the centre of RCW 69 with the 1.0-m MSSSO reflector. The CSPN (arrowed) is close south-east of the brighter of the two stars 11-arcsec apart at the centre of the image which is 3.5 arcmin on a side. The horizontal lines are bad columns on the CCD. North is up and east is left in all panels.

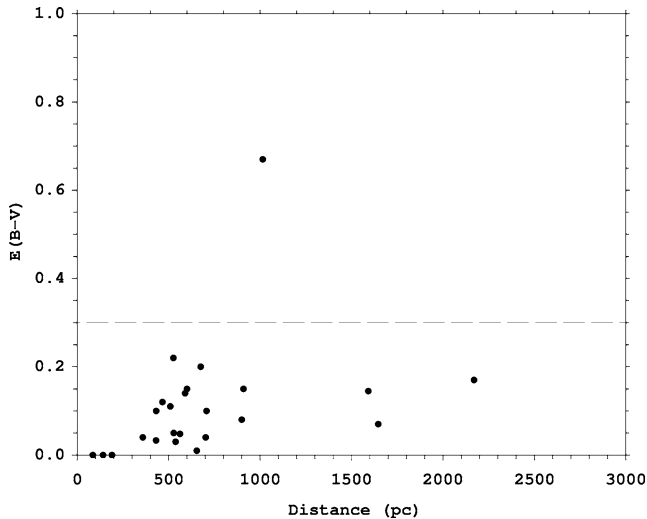


Figure 7. Extinction–distance diagram for the RCW 24 field. The dashed line indicates the reddening value for the PN, $E(B - V) = 0.30$, derived from nebular spectroscopy and the central star colour. Refer to the text.

150–200 pc. Rodgers (1960) determined a distance to the Coalsack of ~ 174 pc, and noted a relatively clear region immediately behind which extended to ~ 1000 pc, beyond which an increase in absorption with distance was noted. Muzzio, Marraco & Feinstein (1974) analysed a region close to RCW 69, and found a general increase in visual absorption from $A_V = 1.0$ at 1300 pc to $A_V = 3.5$ at 2500 pc. This region has also been observed by Seidensticker (1989) and Seidensticker & Schmidt-Kaler (1989). They found that beyond 200 pc in this direction, A_V very slowly increases from 1.0 to 1.5 mag, until $(m - M)_0 = 11.0$ ($D = 1600$ pc), where a steep increase in absorption sets in.

To refine the reddening distance for RCW 69, a search was similarly undertaken in a field of radius 45 arcmin centred on the PN. Data were taken from Seidensticker (1989) where available, supplemented with additional spectroscopic distances as described above. An examination of UKST B and R plates shows this area to lack obvious clouds of heavy absorption, though there is modest differential extinction on small scales as indicated by dust lanes evident across the PN. The closest star to RCW 69 with accurate photometry and spectral typing is HD 110625, 2.5-arcmin north-west of the nebula centre. This star was initially thought to be a possible ionizing source for RCW 69, but was shown by Vogt & Moffat (1975) to be unrelated. Seidensticker (1989) gives a distance of 1320 pc, and this distance is a first-guess estimate for RCW 69, based on the similar reddenings.

Fig. 8 shows the extinction–distance relationship for the RCW 69 field. The increase in extinction at ~ 180 pc corresponds to the near side of the Coalsack complex, and the trend between 180 pc and 3.1 kpc is based on a least-squares fit to the early-type (OBA) stars in the field with best-quality data. The diamond symbols are the open clusters NGC 4609 (Feinstein & Marraco 1971) and Hogg 15 (see the discussion by Piatti et al. 2002). Due to the presence of small-scale absorption variations, the relationship has considerable scatter and a distance of 1200 ± 600 pc for RCW 69 is adopted, based on its observed extinction.

7.2 Kinematic distances

We can derive a standard kinematic distance to RCW 24 based on its observed radial velocity, and assuming it has, like other extreme

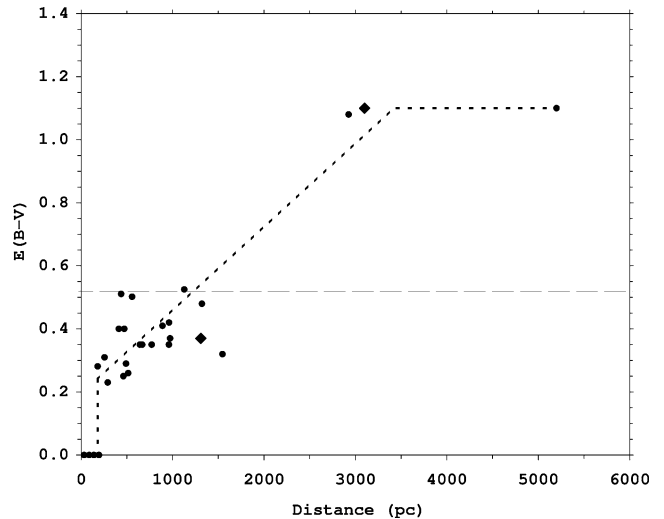


Figure 8. Extinction–distance diagram for the RCW 69 region. The long-dashed line indicates the reddening value for the PN, $E(B - V) = 0.52$, and the short-dashed line is the adopted extinction–distance relationship for the field.

bipolar PNe, a low peculiar velocity relative to its local ISM. We can further justify this assumption, for despite the large size and very low surface brightness of this highly evolved object, there is very little sign of an ISM interaction such as a brighter asymmetric rim or an off-centred central star. Indeed, RCW 24 is one of the lowest surface brightness PNe without any strong evidence of an ISM interaction. Alternatively, the nebula is found in an extremely low-density environment where even a moderate velocity with respect to the ISM will have little effect on the morphology of the PN. However, we consider this scenario unlikely owing to the small z -distance of this PN, well within a disc scaleheight of the interstellar dust and molecular gas (Spitzer 1978).

Our low-dispersion SAAO spectra of RCW 24 are not ideal for radial velocity determination, and have significant associated uncertainties. The observed emission lines give a heliocentric radial velocity of $V_{\text{hel}} = 22 \pm 5 \text{ km s}^{-1}$, derived using the IRAF EMSAO package. The result is an average of the measurements from the individual spectra taken over the two nights. The observations are summarized in Table 4. This translates to $V_{\text{LSR}} = +5 \text{ km s}^{-1}$, which is in reasonable agreement with the CO velocity measured by Brand et al. (1987), but see below. This suggests the CO emission may indeed be intrinsic to the PN, or else it is linked with outlying molecular material of the Vela OB1 association at ~ 1.0 kpc. As a precaution, we use only the optical RV measurements. Using

Table 4. Summary of optical radial velocity determinations for both PNe.

Object ID	Telescope (km s ⁻¹)	V_{hel} (km s ⁻¹)	V_{LSR}
RCW 24	SAAO	$+18 \pm 25$	+1
RCW 24	SAAO	$+26 \pm 28$	+9
RCW 69	UKST/FLAIR	-25.2 ± 8.6	-32.3
RCW 69	UKST/FLAIR	-29.9 ± 4.7	-37.0
RCW 69	SAAO	-20.4 ± 4.6	-27.5
RCW 69	SAAO	-23 ± 17	-30
RCW 69	Marseille FP	–	-22
RCW 69	Marseille FP	–	-48

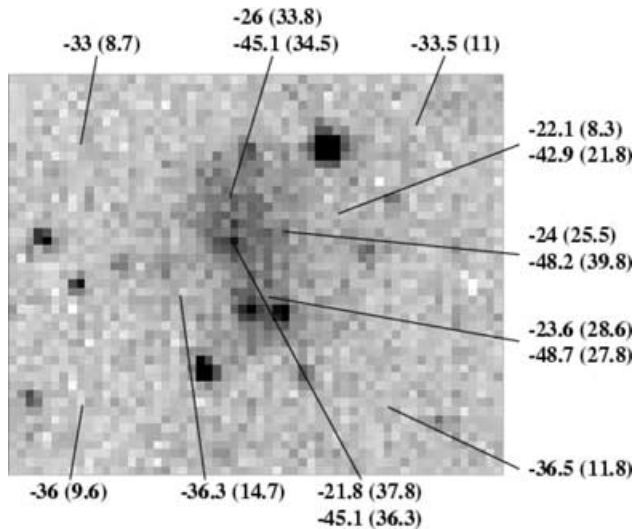


Figure 9. $H\alpha$ image of RCW 69 with the Marseille FP interferometer. Radial velocities (LSR) are indicated with relative intensity values (in arbitrary units) in parentheses. The available data do not allow the internal kinematics to be modelled. The brightest star in the image is HD 110625, which is 2.5 arcmin from the PN centre.

$V_{\text{LSR}} = +5 \text{ km s}^{-1}$ from the optical spectra, the derived kinematic distance is $0.8 \pm 0.8 \text{ kpc}$, the large uncertainty being due to the slow increase in velocity with distance in this direction.

For RCW 69, we combine the FLAIR, and SAAO data to obtain an average velocity of $V_{\text{hel}} = -25.2 \pm 8.6 \text{ km s}^{-1}$ based on the weighted fits to each set of emission lines as provided by the IRAF EMSAO package. A table summarizing the various velocity determinations of each object is given in Table 4.

RCW 69 has also been observed in $H\alpha$ with the Marseille Fabry–Perot (FP) interferometer as part of a study of the spiral structure study of the Galaxy (e.g. Russeil et al. 1998; Russeil 2003). The quite poor spatial resolution (9-arcsec pixel size) relative to the SHS image is seen in Fig. 9. Fortunately, the velocity resolution of the instrument allows us to determine an accurate systemic velocity for the PN. To illustrate this, we present a background-corrected FP $H\alpha$ velocity plot as Fig. 10, which is a profile of the centre of the PN

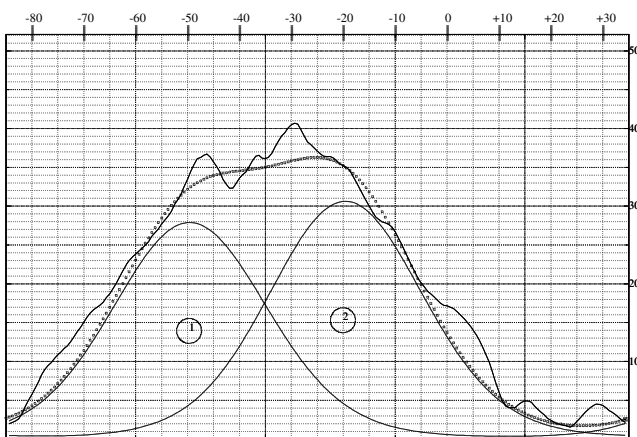


Figure 10. Background-corrected Marseille FP $H\alpha$ spectrum at the centre of RCW 69 in an area of 45 arcsec diameter (similar to the CO data). Velocities in km s^{-1} are given with respect to the LSR and the ordinate plots intensity (in arbitrary units). The overall profile can be modelled by two Gaussian components (refer to the text).

through a 45-arcsec aperture. The $H\alpha$ profile is approximately fit by two Gaussians with mean local standard of rest (LSR) velocities of -22 and -48 km s^{-1} . We interpret these as intrinsic to the PN as these components are absent in a nearby offset field.

The offset field (not illustrated) has components centred at -1 km s^{-1} (Coalsack gas) and $\sim -36 \text{ km s}^{-1}$, which traces the Carina arm, and which is seen to cover the field exterior to the body of the PN (see Fig. 9). The Carina arm in this direction is generally considered to be at 2.5 kpc, but Franco (2000) has used the interstellar Na I D absorption-line profiles to a number of stars near to RCW 69 to suggest the near side of the Carina arm is as close as $D = 0.9\text{--}1.0 \text{ kpc}$ in this direction.

A straight mean of the two intrinsic velocity components of the PN gives a systemic radial velocity of -35 km s^{-1} relative to the LSR. Weighting with the velocities derived from our slit spectra leads to a final systemic velocity of $-33 \pm 3 \text{ km s}^{-1}$. This is, by coincidence, very similar to the diffuse emission tracing the near side of the Carina arm in this direction. Assuming the peculiar velocity of the PN is low (but possibly as high as $\pm 25 \text{ km s}^{-1}$ following Nordström et al. 2004), the standard kinematic distance is $\sim 2\text{--}3 \text{ kpc}$; an earlier estimate by Russeil et al. (1998) placed RCW 69 at 2.1 kpc on the assumption that it was an H II region, following Brand (1986). However, if the near side of the arm is closer, then it may be as near as $\sim 1.0 \text{ kpc}$. Based on the available information, we adopt a kinematic distance of $1.5_{-0.5}^{+1.0} \text{ kpc}$ for RCW 69.

7.2.1 Molecular emission

It has been known for some time that bipolar PNe often have associated molecular H_2 emission (Gatley’s rule: Zuckerman & Gatley 1988; Kastner et al. 1996), and molecular CO emission is also common in bipolar objects (e.g. Huggins & Healy 1989; Huggins et al. 1996). Bipolar PNe are typified by the presence of molecular material, shielded from UV dissociation by either a dense equatorial torus or waist in the PN, or having material in the form of clumpy photodissociation regions. We have therefore considered an a priori assumption that molecular emission is present in these two objects.

Brand et al. (1987) observed RCW 24 in the CO(1–0) line, as part of their kinematic study of the outer Galactic disc. Each lobe was observed separately, with concordant results. They observed a corrected antenna temperature $T_A = 2.4 \text{ K}$, $V_{\text{LSR}} = +12.4 \pm 1.2 \text{ km s}^{-1}$, and mean $\Delta V = 2.3 \text{ km s}^{-1}$ for each lobe. The narrow linewidths of each lobe do not necessarily mitigate against a PN interpretation as Bachiller et al. (1993) observed low linewidths in the lobes of the evolved PN JnEr 1 (= VV 47). However, the measured CO velocities are very similar to those measured in the neighbouring Vela Molecular Ridge (Murphy & May 1991), so the association of the CO with the PN is ambiguous. D. Russeil has observed RCW 69 with the 15-m Swedish-ESO Submillimeter Telescope (SEST). A single pointing in $^{12}\text{CO}(2\text{--}1)$ and $^{12}\text{CO}(1\text{--}0)$ centred on the PN was obtained (Fig. 11; see Russeil & Castets 2004, for further details of the observations). The CO profiles exhibit five distinct lines. The narrow -0.2 and -2.4 km s^{-1} lines are associated with the Coalsack nebula, and there are three broader lines centred at -20.3 , -35.7 and -44.6 km s^{-1} . Brand et al. (1987) also observed RCW 69, and their measured velocities in this direction are identical to our SEST velocities within the uncertainties.

By comparing the CO velocities with the $H\alpha$ spectrum, we consider the -35.7 km s^{-1} line to be associated with the Galactic $H\alpha$ diffuse emission at -36 km s^{-1} which also has a Na I D counterpart (Franco 2000). The -44.6 and -20.3 km s^{-1} lines may be associated

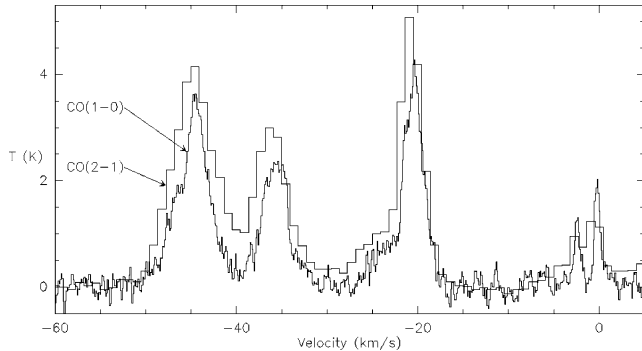


Figure 11. CO(1 – 0) and CO(2 – 1) profiles in the direction of RCW 69.

with the PN. Additionally, the line at -20.3 km s^{-1} shows a clear blueshifted wing which can be fitted with a Gaussian centred at -23.8 km s^{-1} [in CO(1–0), $T = 0.47 \text{ K}$ and $D_v = 3.6 \text{ km s}^{-1}$]. Another blueshifted component is seen in the wing of the -44 km s^{-1} line.

A number of additional CO pointings within 2° of RCW 69 were obtained with SEST. The -36 km s^{-1} component is ubiquitous, and is associated with molecular gas in the near Carina arm. The -20 km s^{-1} CO line is only seen in the direction of the PN, and is probably intrinsic to it. Similarly, the -44 km s^{-1} CO line detected in the direction of RCW 69 matches the velocity of a PN component seen in the FP $H\alpha$ data. However, Na I D interstellar absorption lines at -20 and -40 km s^{-1} are seen towards some stars in this direction (Franco 2000), and furthermore, the CO components have a very high brightness temperature (see Fig. 11), more typical of young, high surface brightness PNe (Huggins et al. 2005). Detailed mapping is thus warranted to confirm beyond doubt if the CO emission is intrinsic or extrinsic to the PN.

The present data do not allow any estimate of the mass of molecular material in either object, assuming the lines are intrinsic to the PNe. We defer this to future workers. Deep imaging at $2.12 \mu\text{m}$ to detect H_2 emission would also be worthwhile to investigate the morphology of these interesting objects. No emission is detected from either PN in the 2MASS K_s band.

7.3 $H\alpha$ surface brightness–radius relation

Another distance technique is the new empirical $H\alpha$ surface brightness–radius relation developed by D. J. Frew and first shown by Pierce et al. (2004). An updated version of this plot is shown in Fig. 12. This new relationship has only become possible due to the availability of accurate $H\alpha$ fluxes, calibrated primarily from the SHASSA southern-sky $H\alpha$ maps (Gaustad et al. 2001). Full details of the calibration will be published elsewhere (Frew & Parker, in preparation). The technique requires an accurate determination of the dimensions of the main body of a PN, excluding any outer haloes (e.g. Corradi et al. 2003). For round and elliptical PNe, the adopted dimensions (used to calculate the mean surface brightness) are easily estimated. However, for bipolar nebulae, estimating the size is generally more difficult, so the surface brightnesses have a greater than average error.

While PNe span more than an order of magnitude in surface brightness at a given radius, a subset of bipolar PNe fall on a tighter trend (see also Frew & Parker 2006) and are seen to be generally larger and hence more massive at a given surface brightness (Fig. 12). For RCW 24, using the dimensions of the main bipolar

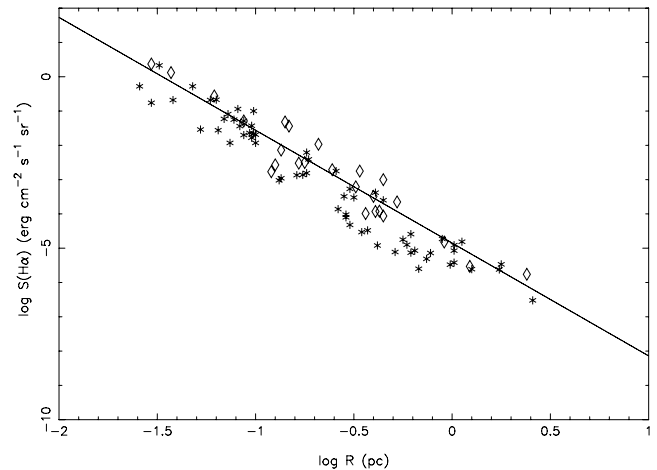


Figure 12. Newly derived $H\alpha$ surface brightness–radius relation based on homogenous flux estimates of a large sample of calibrating PNe. Bipolar PNe are shown as diamonds, and are seen to be generally larger (and hence more massive) at a given surface brightness (see also Frew & Parker 2006). The trend line shown is for the subset of bipolars and is represented by the equation: $\log S(H\alpha) = -3.37(\pm 0.27)\log R - 4.87(\pm 0.19)$.

lobes (excluding the faint outer halo), we estimate $\log S(H\alpha) = -5.24 \text{ erg cm}^{-2} \text{ s}^{-1} \text{ sr}^{-1}$ (corrected for extinction), and a distance, $D = 1.0 \pm 0.4 \text{ kpc}$, while for RCW 69, the corrected $\log S(H\alpha) = -4.24 \text{ erg cm}^{-2} \text{ s}^{-1} \text{ sr}^{-1}$ leads to $D = 1.3 \pm 0.4 \text{ kpc}$.

Phillips (2004) has derived a correlation between the angular diameter and distance to determine distances for 44 bipolar Type I PNe. The implicit assumptions are that bipolar nebulae have similar masses and intrinsic radii. However, bipolar nebulae show a surface brightness relationship with a similar gradient (though offset) to the relationship(s) for round/elliptical PNe (see Fig. 12), refuting Phillips’ assumption. It is clear that there is a distinct trend in these objects, with the torus getting larger with age, as expected from dynamical expansion, and so cannot be used as a ‘standard ruler’. Individual distances of Phillips (2004) are expected to be subject to considerable errors, though statistically the distance scale seems sound.

7.4 Summary of distance determinations

The individual distances obtained above have significant associated errors, but by weighting (by inverse variances) the individual independent values, we derive final adopted distances of $1.0 \pm 0.4 \text{ kpc}$ for RCW 24 and $1.3 \pm 0.4 \text{ kpc}$ for RCW 69. These are the values adopted in Section 10 to investigate the luminosity and mass of the central stars. Both are relatively close, and are well within one scale-height of the plane for bipolar PNe (CF95; Phillips 2001a). The $|z|$ distances from the plane are only ~ 23 and $\sim 7 \text{ pc}$ for RCW 24 and RCW 69, respectively.

8 NEBULAR PARAMETERS

Based on our estimated distance, the main body of RCW 24 subtends $\sim 3.1 \times 2.6 \text{ pc}^2$ and the outer extensions increase the size to $6.4 \times 5.0 \text{ pc}^2$, making this one of the very largest known PNe, even including those with faint, extended haloes (see Corradi et al. 2003). This is a low-excitation nebula based on the strength of the [O III] emission; the excitation class (EC) is only 3 on the scale of Aller (1956), using the measured [O III] line intensities, but a little

higher based on the detection of He II. A decimal excitation class, $EC = 0.8\text{--}1.2$ was calculated according to (equation 2.1a Dopita & Meatheringham 1990). However, the concept of a single number for the excitation class is difficult to quantify for evolved, stratified PNe. These often exhibit significant line-ratio variations at different positions across the nebula, especially with the use of long slits. The EC using equation (2.1b) from Dopita & Meatheringham (1990), which utilizes the He II line strength, was found to vary from 5 to 7 based on the different spectra.

From the rather uncertain $[S\text{II}]\lambda 6717/\lambda 6731$ ratio of 2.0 ± 0.3 (due to the low S/N of these lines), we can only find the limit for $n_e < 10^2\text{ cm}^3$ (Stanghellini & Kaler 1989) since the $[S\text{II}]$ ratio is insensitive to the electron density at this value. Following Pierce et al. (2004), we can determine an approximate rms value of n_e from the observed $H\alpha$ flux, radius and distance according to the relation:

$$n_e^2 = 2.8 \times 10^{22} \frac{F(H\alpha)}{\epsilon \theta^3 d}, \quad (1)$$

where ϵ is the volume filling factor (we assumed $\epsilon = 0.3$, following Pierce et al. 2004), θ is the mean nebular radius in arcsec, and d is the distance in pc. We estimate $n_e = 5\text{ cm}^3$ for RCW 24, which is a very low value. Using simple assumptions, we estimate from the surface brightness of the lobes that $n_e \sim 20\text{ cm}^3$ at the position of each slit. Following Pottasch (1996), the ionized mass is given by

$$M = 4.03 \times 10^{-4} \epsilon^{1/2} d^{5/2} (H\beta)^{1/2} \theta^{3/2} M_\odot, \quad (2)$$

where d is the distance in kpc and $H\beta$ is the reddening-corrected flux in units of $10^{-11}\text{ erg cm}^{-2}\text{ s}^{-1}$. For RCW 24, the ionized mass of the main body of the PN is $\sim 0.8 M_\odot$, considerably greater than the canonical PN Shklovsky mass of $0.2 M_\odot$. Including the outer dimensions, the ionized mass is predicted to be substantially above $1 M_\odot$.

The $[O\text{III}]$ apparent magnitude of RCW 24 is $m_{5007} = 14.0 \pm 0.6$. This was calculated from the observed flux (see Section 5) and the formula of Jacoby (1989). Using the adopted distance and the extinction $A_{5007} = 1.06$, derived using the Howarth (1983) reddening law, the absolute magnitude is $M_{5007} = +2.9 \pm 0.6$. This is ~ 7.5 mag down the PN luminosity function from the brightest PNe (e.g. Ciardullo 2005), attesting to the very evolved nature of this object.

RCW 69 also has a relatively large intrinsic diameter, with dimensions of the main body of the PN being $1.6 \times 1.5\text{ pc}^2$. For RCW 69, the excitation class is in general higher than RCW 24, with stronger $[O\text{III}]$ and He II emission. This is not unexpected as the reddening-corrected surface brightness is greater for this less-evolved PN. We determine $EC = 4\text{--}5$ on the scale of Aller (1956) and $EC \simeq 2$ and $EC = 6\text{--}7$ using the two equations of Dopita & Meatheringham (1990). Again it is not possible to derive a single value for the excitation class for this evolved PN.

As before we use the $[S\text{II}]$ line ratio to estimate n_e . The unfluxed FLAIR and flux-calibrated red SAAO spectra gave $[S\text{II}]\lambda 6717/\lambda 6731 \sim 1.27$ and ~ 1.28 , respectively, from well-resolved lines. The lower-dispersion SAAO spectra yield $[S\text{II}]\lambda 6717/\lambda 6731 \sim 1.04$ and ~ 1.34 for data of lower S/N and poorer resolution. The electron densities range from <100 to $\sim 450\text{ cm}^3$ for the different spectra, which can be compared to the derived rms density for the whole nebula assuming a volume filling factor of 0.3, $n_e = 35\text{ cm}^3$. We use a density of 250 cm^3 (from a weighted average of the spectra) and an electron temperature of $10\,300\text{ K}$ from the measured $\lambda 5755/\lambda 6584$ ratio to determine the abundances in Section 9 below. It follows that the ionized nebular mass is $\sim 0.5 M_\odot$.

The apparent and absolute $[O\text{III}]$ magnitudes are $m_{5007} = 13.8 \pm 0.5$ and $M_{5007} = +1.4 \pm 0.6$, determined in the same way as for

RCW 24. RCW 69 is also a rather faint PN, though more luminous and less evolved than RCW 24.

9 CHEMICAL ABUNDANCES

The definition of a PN of Type I has changed since the original investigations of Peimbert (1978) and Peimbert & Serrano (1980). PTP83 classified Type I PNe as having $\text{He}/\text{H} \geq 0.125$ and $\log(\text{N}/\text{O}) \geq -0.3$ on the basis of improved data. (hereafter KSK90 Kaler, Shaw & Kwitter 1990) adopted $\text{He}/\text{H} > 0.15$ and $\log(\text{N}/\text{O}) \geq -0.1$ for Type I PNe. KB94 have formalized the definition, regarding a Type I PN as being produced by a progenitor star in which envelope-burning conversion of dredged-up primary carbon to nitrogen has occurred. The associated PN will therefore have a nitrogen abundance that exceeds the initial C+N abundance of the progenitor star. This abundance can be inferred from the average C+N abundance of an ensemble of local H II regions, which is a reasonable assumption excluding thick-disc or halo PNe (both PNe discussed here are thin-disc objects). For the nearby Galactic neighbourhood, this corresponds to $\log(\text{N}/\text{O}) \geq -0.1$. KB94 find a large range in the He/H ratio for nitrogen-enhanced PNe and have consequently not used this criterion for differentiating Type I PNe. We will use their definition in the discussion that follows.

We conducted a preliminary interpretation of the nebular spectrum of RCW 24, using the plasma diagnostics code HOPPLA (Acker et al. 1989; Köppen, Acker & Stenholm 1991). Both spectra are of low S/N so no line ratios for the electron temperature are available; we assume a value of 10^4 K . Perinotto & Corradi (1998) found that $T_e[\text{N II}]$ is usually higher than $T_e[\text{O III}]$ for bipolar PNe (however, see the discussion by McKenna et al. 1996). In the absence of temperature diagnostics, we formally set $T_e[\text{O III}] = T_e[\text{N II}]$ and note that the derived abundances have a larger than average uncertainty.

The $[S\text{II}]$ doublet ratio is in the low-density limit, and we have used a density of 20 cm^{-3} (see Section 8). Since this is a low-density PN, the line strengths are not affected by collisional de-excitation, so the derived abundances are essentially independent of our assumed n_e value. However, we cannot derive an accurate flux estimate for the $[O\text{II}]$ doublet from either spectrum, so only an approximate N/O value can be determined. The data are insufficient to determine an accurate He/H ratio for RCW 24. The results are collected in Table 5.

For RCW 69, the abundances generally have higher weight due to the better S/N of the available spectra. Helium appears to be enhanced above solar ($\text{He}/\text{H} = 0.29$) but the abundance has a significant error, since the He I $\lambda 5876$ flux is uncertain. The calculated $\log(\text{N}/\text{O})$ ratio is $+0.33\text{ dex}$ ($\text{N}/\text{O} = 2.1$), classifying it as a bona fide Type I PN according to KB94. An alternative method is to use the precepts of Kaler (1983), and derive a simple expression for N/O based on the well-known fact that the ionization potentials for O^+ and N^+ are similar. At $T_{\text{eff}} = 10\,000\text{ K}$, equation (5) of Kaler (1983)

Table 5. Elemental abundances by number for the two PNe, given in the usual notation of $12 + \log[n(\text{X})/n(\text{H})]$. The abundances for Type I and non-Type I PNe and solar abundances are taken from KB94. Both PNe are strongly enhanced in nitrogen.

Element	RCW 24	RCW 69	Type I	non-Type I	Solar
He	>10.96	11.46:	11.11	11.05	10.99
N	8.47	8.70	8.72	8.14	8.00
O	8.03:	8.37	8.65	8.69	8.93
S	6.82:	6.94	6.91	6.91	7.24
Ar	–	6.30:	6.42	6.38	–
$\log(\text{N}/\text{O})$	0.44:	0.33	0.07	–0.55	–0.93

reduces to

$$\frac{N}{O} = 0.52 \frac{I(6584)}{I(3727)}. \quad (3)$$

For RCW 69, we determine $\log(N/O) = +0.35$, which agrees well with the value of $+0.33$ from plasma diagnostics. Though the quality of the available spectra do not allow more than a first estimate of the elemental abundances, both are seen to be Type I PNe, with strongly enhanced nitrogen abundances. The He abundance for RCW 69 is also enhanced above solar. Deeper spectra are needed to obtain more accurate estimates of the elemental abundances.

10 CENTRAL STAR PROPERTIES

The central star of RCW 24 has $V = 18.21$. Using our preferred distance of 1.0 kpc and a reddening of $E(B - V) = 0.30$, allows the absolute magnitude to be determined as $M_V = 7.3 \pm 0.7$. Similarly for RCW 69 $M_V = 6.3 \pm 0.5$. These values are consistent with Phillips (2005) who found an average absolute magnitude of $M_V \geq 7.05 \pm 0.26$ for a number of evolved CSPN.

Several methods are in use to determine the temperatures of the ionizing stars of PNe. The classical Zanstra method requires an integrated nebular flux in a Balmer Line (usually $H\beta$) and a B or V magnitude for the central star, assuming the nebula is optically thick in the Lyman continuum. A blackbody spectrum is also assumed for the CS, following Pottasch (1984). A helium Zanstra temperature can also be calculated given the integrated flux in the $He\ II \ \lambda 4686$ line. For RCW 24, H and He Zanstra temperatures were determined following the formulation of Pottasch (1984). Using the $H\beta$ flux, we estimate $T_z(H\ I) = 95 \pm 8$ kK. This is a probable lower limit since the geometric filling factor, ξ (Harman & Seaton 1966; Kaler 1983), is almost certainly less than unity, based on the observed morphology of the PN (i.e. the PN is optically thin in some directions). The helium Zanstra temperature is 121 ± 20 kK, the large uncertainty following from the poorly estimated $\lambda 4686$ flux.

Since the magnitude of the CSPN of RCW 69 is only approximate, the Zanstra temperatures for RCW 69 are also fairly uncertain. We estimate $T_z(H\ I) = 106 \pm 12$ kK, and $T_z(He\ II) \leq 128 \pm 15$ kK.

In addition, crossover (Ambartsumyan) temperatures (Kaler & Jacoby 1989) can be determined for both objects. This method calculates a temperature (and CSPN magnitude) by forcing agreement between the H and He Zanstra temperatures, and necessarily assumes that the nebula is optically thick. Using equation (1) of Kaler & Jacoby (1989), we derive $T_{\text{cross}} = 146^{+37}_{-32}$ kK for RCW 24 and $T_{\text{cross}} = 164^{+30}_{-20}$ kK for RCW 69. These estimates will be refined following a better determination of the $He\ II$ flux for each PN, but are at least consistent with the Zanstra determinations. Given the errors on these determinations, we quote temperature estimates of ~ 120 kK for RCW 24 and ~ 130 kK for RCW 69.

By applying representative bolometric corrections (e.g. Schönberner 1981; Vacca, Garmany & Shull 1996), we estimate the luminosity of the CSPN in RCW 24 as $70^{+80}_{-40} L_{\odot}$ and $190^{+90}_{-80} L_{\odot}$ for the CSPN in RCW 69. By interpolating between standard post-AGB evolutionary tracks, it is possible to estimate masses for the central stars of PNe. However, as the errors on both the temperatures and luminosities of both central stars are substantial, our derived masses are very uncertain. Furthermore, at these low luminosities the evolutionary tracks are crowded. Nevertheless, by comparison with the post-AGB hydrogen burning evolutionary tracks of Blöcker (1995), both central star masses are likely to be greater than $0.60 M_{\odot}$. More accurate values will follow from a better determination of the stellar temperatures. Both nuclei

appear to quite hot and somewhat more massive than the canonical mean for hot white dwarfs of $\sim 0.56 M_{\odot}$ (e.g. Vennes et al. 1997; Madej, Należyty & Althaus 2004).

11 DISCUSSION

Two large, low surface brightness nebulae, previously identified as $H\ II$ regions, have been reclassified as evolved bipolar planetary nebulae. Both PNe have originated from fairly massive progenitors (> 2.0 – $2.5 M_{\odot}$), deduced from their large ionized masses, Type I chemistries, small $|z|$ distances, low peculiar velocities and relatively hot (and massive?) central stars. They are an important addition to the small sample of evolved bipolar PNe in the solar neighbourhood.

Within a volume of radius 1.0 kpc, only seven or eight objects are definite Type I PNe following KB94 (Frew & Parker, in preparation). These are Abell 21, Abell 24, Abell 29, Abell 71, M 1–41, He 2–11 and RCW 24, plus NGC 6302 (Meaburn et al. 2005). The extremely evolved object WDHS 1 is also a probable Type I PN, based on a spectrum obtained by us. Seven more PNe, NGC 7293, M 27 (NGC 6853), M 57 (NGC 6720), NGC 2346, NGC 6781, Sh 2–188, and JnEr 1, have been classified as Type I nebulae by various workers (e.g. Rosado & Kwitter 1982; Bohigas 2001, 2003; Perinotto, Morbidelli & Scatarzi 2004), but these all have N/O ratios below the KB94 cut-off. Data for YM 16, and Abell 45 are being analysed to see if they are also nearby Type I PNe (Frew & Parker, in preparation).

Based on the number of nearby Type I PNe, we conclude that only ~ 10 per cent of the local 1-kpc sample has Type I chemistries. Further work to refine this estimate is ongoing (Frew & Parker, in preparation), based on larger though less complete ‘1.5-’ and ‘2-kpc’ samples, with the goal of refining the total number, scaleheight and birth rate of bipolar (and/or Type I) PNe in the Galaxy. We leave this work to future papers in this series.

ACKNOWLEDGMENTS

We gratefully thank Patrick Woudt who provided UBV photometry of the CS in RCW 24. This study used data from the AAO/UKST $H\alpha$ survey with the support of the Anglo-Australian Telescope Board and the Particle Physics and Astronomy Research Council (U.K.), and from the SHASSA, which was produced with support from the National Science Foundation. This research has made use of the SIMBAD data base, operated at the CDS, Strasbourg, France. DJF and QAP acknowledge the support of ANSTO to enable them to undertake the spectroscopic observations. Technical support from Brent Miszalski is gratefully acknowledged, and Greg Madsen, Patrick Huggins and Albert Zijlstra provided useful discussions. We also thank the referee, Romano Corradi, for constructive comments that improved the form and content of this paper.

REFERENCES

- Acker A., Köppen J., Stenholm B., Jasiewicz G., 1989, *A&AS*, 80, 201
- Aller L. H., 1956, *Gaseous Nebulae*. Chapman & Hall, London
- Bachiller R., Huggins P. J., Cox P., Forveille T., 1993, *A&A*, 267, 177
- Becker S. A., Iben I., 1980, *ApJ*, 237, 11
- Bergeron P., Wesemael F., Beauchamp A., 1995, *PASP*, 107, 1047
- Blöcker T., 1995, *A&A*, 299, 755
- Bohigas J., 2001, *RMxAA*, 37, 237
- Bohigas J., 2003, *RMxAA*, 39, 149
- Brand J., 1986, Unpublished PhD thesis, Univ. of Leiden
- Brand J., Blitz L., Wouterloot J. G. A., 1986, *A&AS*, 65, 537
- Brand J., Blitz L., Wouterloot J. G. A., Kerr F. J., 1987, *A&AS*, 68, 1

- Brocklehurst M., 1971, *MNRAS*, 153, 471
- Ciardullo R., 2005, in *Szczerba R., Stasinska G., Gorny S., eds, AIP Conf. Proc. Vol. 804, Planetary Nebulae as Astronomical Tools*. Springer, New York, p. 277
- Copetti M. V. F., 2000, *A&AS*, 147, 93
- Corradi R. L. M., 1995, *A&A*, 276, 521
- Corradi R. L. M., Schwarz H. E., 1993, *A&A*, 268, 714
- Corradi R. L. M., Schwarz H. E., 1995, *A&A*, 293, 871 (CS95)
- Corradi R. L. M., Villaver E., Mampaso A., Perinotto M., 1997, *A&A*, 324, 276
- Corradi R. L. M., Brandi E., Ferrer O. E., Schwarz H. E., 1999, *A&A*, 343, 841
- Corradi R. L. M., Schönberner D., Steffen M., Perinotto M., 2003, *MNRAS*, 340, 417
- Dopita M. A., Hua C. T., 1997, *ApJS*, 108, 515
- Dopita M. A., Meatheringham S. J., 1990, *ApJ*, 357, 140
- Feinstein A., Marraco H. G., 1971, *PASP*, 83, 218
- Fitzgerald M. P., 1968, *AJ*, 73, 983
- Franco G. A. P., 2000, *MNRAS*, 315, 611
- Frew D. J., 1997, *South. Astron.*, 2, 6
- Frew D. J., Parker Q. A., 2003, *AAONw*, 103, 6
- Frew D. J., Parker Q. A., 2005, in *Szczerba R., Stasinska G., Gorny S., eds, AIP Conf. Proc. Vol. 804, Planetary Nebulae as Astronomical Tools*. Springer, New York, p. 11
- Frew D. J., Parker Q. A., 2006, in *Barlow M. J., Mendez R. H., eds, IAU Symp. 234, Planetary Nebulae in our Galaxy and Beyond*. Cambridge Univ. Press, Cambridge, in press
- Gaustad J. E., McCullough P. R., Rosing W., Van Buren D. J., 2001, *PASP*, 113, 1326
- Greig W. E., 1967, *AJ*, 72, 801
- Greig W. E., 1971, *A&A*, 10, 161
- Gum C. S., 1955, *MNRAS*, 67, 155
- Hambly N. et al., 2001, *MNRAS*, 326, 1279
- Harman R. J., Seaton M. J., 1966, *MNRAS*, 132, 15
- Howarth I. D., 1983, *MNRAS*, 203, 301
- Hua C. T., 1997, *A&AS*, 125, 355
- Huggins P. J., Healy A. P., 1989, *ApJ*, 346, 201
- Huggins P. J., Bachiller R., Cox P., Forveille T., 1996, *A&A*, 315, 284
- Huggins P. J., Bachiller R., Planesas, P., Forveille T., Cox P., 2005, *ApJS*, 160, 272
- Iben I., 1995, *Phys. Rep.*, 250, 2
- Jacoby G. H., 1989, *ApJ*, 339, 39
- Kaler J. B., 1983, *ApJ*, 271, 188
- Kaler J. B., Jacoby G. H., 1989, *ApJ*, 345, 871
- Kaler J. B., Shaw R. A., Kwitter K. B., 1990, *ApJ*, 359, 392 (KSK90)
- Kastner J. H., Weintraub D. A., Gatley I., Merrill K. M., Probst R. G., 1996, *ApJ*, 462, 777
- Kingsburgh R. L., Barlow M. J., 1994, *MNRAS*, 271, 257 (KB94)
- Köppen J., Acker A., Stenholm B., 1991, *A&A*, 248, 197
- Lucke P. B., 1978, *A&A*, 64, 367
- Lynga G., 1965, *Lund Medd. Astron. Obs. Ser. II*, 142, 1
- Madej J., Należyty M., Althaus L. G., 2004, *A&A*, 419, L5
- Manchado A., Guerrero M. A., Stanghellini L., Serra-Ricart M., 1996, *The IAC Morphological Catalog of Northern Galactic Planetary Nebulae*. Instituto de Astrofísica de Canarias, La Laguna, Spain
- May J., Alvarez H., Bronfman L., 1997, *A&A*, 327, 325
- McKenna F. C., Keenan F. P., Kaler J. B., Wickstead A. W., Bell K. L., Aggarwal K. M., 1996, *PASP*, 108, 610
- Meaburn J., López J. A., Steffen W., Graham M. F., Holloway A. J., 2005, *AJ*, 130, 2303
- Morgan D. H., Parker Q. A., 1998, *MNRAS*, 296, 921
- Muzzio J. C., Marraco H. G., Feinstein A., 1974, *PASP*, 86, 394
- Murphy D. C., May J., 1991, *A&A*, 247, 202
- Neckel T., Klare G., 1980, *A&AS*, 42, 251
- Neckel T., Vehrenberg H., 1990, *Atlas Galaktischer Nebel, Teil III*. Verlag K. G., Treugesell
- Nordström B., Mayor M., Andersen J. et al., 2004, *A&A*, 418, 989
- Parker Q. A., 1997, in *Kontizas M., Kontizas D. H., Morgan D. H., Vettolani G. P., eds, Proc. 2nd Conf. Working Group, IAU Comm. 9, ASSL, Vol. 212, Kluwer, Dordrecht*, p. 25
- Parker Q. A. et al., 2001, *The Edinburgh/AAO/Strasbourg Catalogue of Galactic PN: Preliminary Version 1.0 on CD-ROM*
- Parker Q. A. et al., 2003, in *Dopita M., Kwok S., Sutherland R., eds, ASP Conf. Ser. Vol. 209, Planetary Nebulae and Their Role in the Universe*. Astron. Soc. Pacific, San Francisco, p. 41
- Parker Q. A. et al., 2005, *MNRAS*, 362, 689
- Parker Q. A. et al., 2006, *MNRAS*, in press
- Peimbert M., 1978, in *Terzian Y., ed., IAU Symp. Vol. 76, Planetary Nebulae: Observations and Theory*. D. Reidel, Dordrecht, p. 215
- Peimbert M., Serrano A., 1980, *RMxAA*, 5, 9
- Peimbert M., Torres-Peimbert S., 1983, in *Flower D. R., ed, IAU Symp. Vol. 103, Planetary Nebulae*. Dordrecht, Reidel, p. 233 (PTP83)
- Perinotto M., Corradi R. L. M., 1998, *A&A*, 332, 721
- Perinotto M., Morbidelli L., Scatarzi A., 2004, *MNRAS*, 349, 793
- Pettersson B., Reipurth B., 1994, *A&AS*, 104, 233
- Piatti A. E., Bica E., Santos J. F. C. Jr., Clariá J. J., 2002, *A&A*, 387, 108
- Pierce M. J., Frew D. J., Parker Q. A., Köppen J., 2004, *PASA*, 21, 334
- Phillips J. P., 2001a, *MNRAS*, 326, 1041
- Phillips J. P., 2001b, *PASP*, 113, 846
- Phillips J. P., 2004, *New Astron.*, 9, 391
- Phillips J. P., 2005, *MNRAS*, 357, 619
- Pottasch S. R., 1984, *Planetary Nebulae*. D. Reidel, Dordrecht
- Pottasch S. R., 1996, *A&A*, 307, 561
- Riesgo-Tirado H., López J. A., 2002, *RMxAA (Serie de Conf.)*, 12, 174
- Rodgers A. W., 1960, *MNRAS*, 120, 163
- Rodgers A. W., Campbell C. T., Whiteoak J. B., 1960a, *MNRAS*, 121, 103
- Rodgers A. W., Campbell C. T., Whiteoak J. B., Bailey H. H., Hunt V. O., 1960b, *An Atlas of H-Alpha Emission in the Southern Milky Way*. Australian National University, Canberra
- Rosado M., Kwitter K. B., 1982, *RMxAA*, 5, 217
- Russeil D., 2003, *A&A*, 397, 133
- Russeil D., Castets A., 2004, *A&A*, 417, 107
- Russeil D., Georgelin Y. M., Amram P., Gach J. L., Georgelin Y. P., Marcelin M., 1998, *A&AS*, 130, 119
- Schmidt-Kaler T., 1982, *Landolt-Börnstein, New Series, Group VI*, 2, 1
- Schlegel D. J., Finkbeiner D. P., Davis M., 1998, *ApJ*, 500, 525
- Schönberner D., 1981, *A&A*, 103, 119
- Seidensticker K. J., 1989, *A&AS*, 79, 61
- Seidensticker K. J., Schmidt-Kaler Th., 1989, *A&A*, 225, 192
- Soker N., 1998, *ApJ*, 496, 833
- Spitzer L., 1978, *Physical Processes in the Interstellar Medium*. Wiley-Interscience, New York
- Stanghellini L., Kaler J. B., 1989, *ApJ*, 343, 811
- Stone R. P. S., Baldwin J. A., 1983, *MNRAS*, 204, 347
- Tylenda R., 1989, in *Torres-Peimbert S., ed, IAU Symp. Vol. 131, Planetary Nebulae*. Kluwer, Dordrecht, p. 175
- Vacca W. D., Garmany C. D., Shull J. M., 1996, *ApJ*, 460, 914
- Vennes S., Thejll P., Galvan R. G., Dupuis J., 1997, *ApJ*, 480, 714
- Vogt N., Moffat A. F. J., 1975, *A&A*, 45, 405
- Watson F. G., Gray P., Oates A. P., Lankshear A., Dean R. G., 1993, in *Gray P. M., ed., ASP Conf. Ser. Vol. 37, Fibre Optics in Astronomy II*. Astron. Soc. Pac., San Francisco, p. 171
- Zuckerman B., Gatley I., 1988, *ApJ*, 324, 501

This paper has been typeset from a $\text{\TeX}/\text{\LaTeX}$ file prepared by the author.